IEEE Access
Multidisciplinary | Rapid Review | Open Access Journal

Received April 29, 2020, accepted May 3, 2020, date of publication May 6, 2020, date of current version May 20, 2020.

Digital Object Identifier 10.1109/ACCESS.2020.2992663

Adaptive Event-Triggered Load Frequency Control of Multi-Area Power Systems Under Networked Environment via Sliding Mode Control

XINXIN LV[1,2], (Student Member, IEEE), YONGHUI SUN[1], (Member, IEEE), YI WANG[1], (Student Member, IEEE), AND VENKATA DINAVAHI[2], (Fellow, IEEE)

[1]College of Energy and Electrical Engineering, Hohai University, Nanjing 210098, China
[2]Department of Electrical and Computer Engineering, University of Alberta, Edmonton, AB T6G 2V4, Canada

Corresponding author: Yonghui Sun (sunyonghui168@gmail.com)

This work was supported in part by the National Natural Science Foundation of China under Grant 61673161, in part by the Fundamental Research Funds for the Central Universities under Grant 2019B67414, in part by the Six Talent Peaks High Level Project of Jiangsu Province under Grant 2017-XNY004, in part by the Innovation Team of Six Talent Peaks Project of Jiangsu Province under Grant 2019-TD-XNY-001, and in part by the Natural Science and Engineering Research Council (NSERC) of Canada. The work of Xinxin Lv was supported by the China Scholarship Council.

ABSTRACT The robust stability and stabilization of adaptive event-triggered load frequency control (LFC) with sliding mode control (SMC) for multi-area power systems under a networked environment are investigated in this paper. The adaptive event-triggered scheme is proposed to maximize network bandwidth utilization, and it can be adaptively modified according to circumstances. Furthermore, to provide stronger robustness performance which is against the frequency deviation induced by power unbalance or transmission time delays, the SMC is developed. Then, the LFC scheme for multi-area power systems under the networked environment is modeled as a Markov jump linear system model, to describe the uncertainty parameters and external disturbances better in this system. Additionally, by employing Wirtinger-based inequality and Lyapunov theory, the robust stability and stabilization criteria with less conservatism are derived. Finally, simulations are performed to demonstrate the efficacy and superiority of the developed approach.

INDEX TERMS Adaptive event-triggered scheme, load frequency control, networked communication, sliding mode control, Wirtinger-based inequality.

I. INTRODUCTION

To operate a power system with sufficient supply and reliability, it is significant to make the power generation corresponds to the power demand during variations in load and source [1]–[3]. The load frequency control (LFC) plays thus a critical role in mitigating unwanted tie-line power flows and frequency variations between neighboring interconnected areas [4], [5]. The LFC scheme explicitly aims to ensure zero steady-state errors for frequency and tie-line input flows of power systems [6], [7]. Therefore, holding the power system steady and secure is a very important process. At the same time, the investigation of LFC in power systems can be treated as the research of objective optimization and robust control.

The associate editor coordinating the review of this manuscript and approving it for publication was Shihong Ding.

In modern power systems, dedicated communication channels and open communication infrastructure are the popular methods to connect neighboring contact areas [8], [9]. Modern power systems with open communication networks are competitive compared to conventional power systems with dedicated communication channels. At the same time, it has lower costs and greater flexibility [10]. However, along with it come the finite communication time delays, packet dropouts, and disordering [11]. Hence, some new challenges have been present for the power systems. More importantly, since multi-area power systems are growing rapidly, so the limited communication and computational resources are congested by higher load data transfers. Therefore, the problem of limited network utilization is becoming more and more severe.

The event-triggered scheme has recently become a focus area for the modern power system with open communication networks to save network bandwidth and minimize

transmission frequency. For the event-triggered scheme, the data packets of the sampled signals can be transmitted only when the designed triggering criterion is satisfied [12]. In this way, the unnecessary use of computational and networking resources can be reduced and the use of network bandwidth maximized. Therefore, the event-triggered scheme has been applied in various fields, for instance, networked systems [13], [14], multi-agent systems [15], [16] as well as the LFC scheme for power systems [17], and some representative results have been demonstrated. The communication delays and event-triggered scheme were incorporated for the LFC scheme in [18]; the event-triggered LFC scheme including supplementary adaptive dynamic programming was presented in [19]; as well as based on the event-triggered communication, the distributed reactive power sharing control was studied [20]. However, the above researches about the event-triggered scheme are all predesigned. To improve this and save more network utilization, the adaptive event-triggered scheme [21], [22] in which the event-triggered threshold can be adaptively modified according to the previous and present transmitted signal packets is investigated in this paper.

Sliding mode control (SMC), with fast response and robust performance, is a control strategy to guarantees power system high robust performance [18], [23], [24]. Under load disturbance, the control process of frequency and tie-line power deviations may become very challenging. It is well known that the SMC procedure demands that specified switching surfaces be built and a controller synthesized [25]. Depending on this the trajectories of the state can be forced to move in a finite time towards the sliding mode surface, which can improve the system transient performance greatly [26], [27]. Thus, it has been widely utilized in engineering practice, especially in the LFC scheme. For example, the robust stabilization of the LFC scheme with the SMC approach was proposed in [28]; the sliding mode LFC for hybrid power system was studied in [29]; and the robust SMC of wind energy conversion systems were investigated in [30]. Therefore, to solve frequency problems, the SMC strategy is proposed in this paper.

In particular, Markov jump systems can be utilized to model abrupt variations caused by device failures, sudden environmental changes, changing interconnections with subsystems [32], [33]. Multiple practical systems, such as solar boiler stations, economics, dc motor units, RLC circuits, can be modeled as Markov jump system [34]. Also, it is composed of several interacting operating modes and a dynamic mechanism involving stochastic hopping, which is ultimately controlled by a Markov chain [35]. Hence, taking the uncertain model parameters and external disturbances caused by the complexity of the power system model and various environments, the Markov model is applied in this paper.

Motivated by the debates above, this paper investigates the LFC scheme combining adaptive event-triggered strategy and SMC for power systems operated over a bandwidth-limited communication channel. In open communication networks, the transmission time delay is the inevitable factor destroying the system performance. Hence, the transmission time delay is considered in this paper. To save more network bandwidth utilization, the adaptive event-triggered scheme is applied in this paper. At the same time, considering the increase in renewable energy sources, the wind power has been integrated into the proposed system model [26], [31]. Additionally, the SMC strategy is employed to guarantee the power system's robust performance which will be caused by external disturbances and parameter variation. Specifically, taking the uncertain parameters and external disturbances, the Markov model is proposed in this paper. By utilizing Lyapunov theory, the criteria of stability and stabilization for the power system can be deduced in terms of linear matrix inequality (LMI). Specifically, through the Wirtinger-based inequality, the less conservative conditions of them can be obtained. The main contribution of this study is three-fold:

1) In multi-area power systems, higher load data transfer congested restricted communication and computing resources. To improve the limited network bandwidth utilization and save more network resources, the adaptive event-triggered scheme is applied. In this scheme, the adaptive threshold is considered which can be adaptively modified according to the previous and present transmitted signal packets.
2) The stability of the power grid is vitally necessary. It should be noted that SMC has the advantage of fast response and robust performance. Thus, to improve the robust performance of the power system, the SMC strategy is employed in this paper.
3) By exploiting a suitable Lyapunov function and Wirtinger-based inequality, the controller design strategies and stability conditions with an H_∞ attenuation level $\gamma > 0$ are studied under less conservative condition.

The remainder of this paper is structured as follows. Section II introduces the model of the LFC scheme which involves adaptive event-triggered scheme and SMC strategy with transmission time delays. Then, by using the Wirtinger-based inequality and Lyapunov theory, the asymptotically stable condition with H_∞ performance and robust controller design results are investigated in Section III. Section IV demonstrates numerical results to express the effectiveness of the method presented in this paper. Eventually, this work is concluded in Section V.

II. PROBLEM STATEMENT

The multi-area power system is presented in Fig.1, which contains the adaptive event-triggered scheme and sliding mode control strategy. The notations of the i-th control area are given in Table 1. The multi-area power system model can generally be represented by a linear time-invariant system as follows:

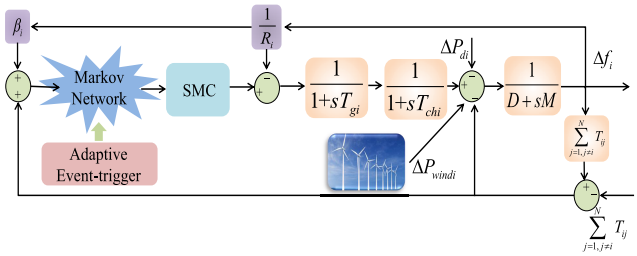

FIGURE 1. Transfer function model of multi-area time-delay hybrid power system.

TABLE 1. Notations.

Symbol	Quantity
ΔP_{di}	Load deviation
ΔP_{mi}	Generator mechanical output deviation
ΔP_{vi}	Valve position deviation
ΔP_{windi}	Out of wind turbine generator deviation
Δf_i	Frequency deviation
ΔP_{tie-i}	tie-line active power deviation
M_i	Moment of inertia
D_i	Generator damping coefficient
T_{gi}	Time constant of the governor
T_{chi}	Time constant of the turbine
R_i	Speed drop
β_i	Frequency bias factor
T_{ij}	Tie-line synchronizing coefficient

$$\begin{cases} \dot{x}(t) = Ax(t) + Bu(t) + F\omega(t) \\ y(t) = Cx(t) \end{cases} \tag{1}$$

where

$$x_i(t) = \begin{bmatrix} \Delta f_i & \Delta P_{mi} & \Delta P_{vi} & \int ACE_i & \Delta P_{tie-i} \end{bmatrix}^T$$
$$x(t) = \begin{bmatrix} x_1(t)^T & x_2(t)^T & \dots & x_N(t)^T \end{bmatrix}^T$$
$$y_i(t) = ACE_i, \omega_i(t) = \begin{bmatrix} \Delta P_{di} & \Delta P_{windi} \end{bmatrix}^T$$
$$y(t) = \begin{bmatrix} y_1(t)^T & y_2(t)^T & \dots & y_N(t)^T \end{bmatrix}^T$$
$$\omega(t) = \begin{bmatrix} \omega_1(t)^T & \omega_2(t)^T & \dots & \omega_N(t)^T \end{bmatrix}^T$$
$$A_{ii} = \begin{bmatrix} \frac{-D_i}{M_i} & \frac{1}{M_i} & 0 & 0 & \frac{-1}{M_i} \\ 0 & \frac{-1}{T_{chi}} & \frac{1}{T_{chi}} & 0 & 0 \\ \frac{-1}{RT_{g_i}} & 0 & \frac{-1}{T_{g_i}} & 0 & 0 \\ \beta_i & 0 & 0 & 0 & 1 \\ 2\pi \sum_{j=1, j\neq i}^{N} T_{ij} & 0 & 0 & 0 & 0 \end{bmatrix}$$
$$A_{ij} = \begin{bmatrix} (5,1) = -2\pi T_{ij} \end{bmatrix}$$

$$A = \begin{bmatrix} A_{11} & A_{12} & \dots & A_{1N} \\ A_{21} & A_{22} & \dots & A_{2N} \\ \vdots & \vdots & \ddots & \vdots \\ A_{N1} & A_{N2} & \dots & A_{NN} \end{bmatrix}$$
$$B_i = \begin{bmatrix} 0 & 0 & \frac{1}{T_{gi}} & 0 & 0 \end{bmatrix}^T$$
$$B = diag\{ B_1 \quad B_2 \quad \dots \quad B_N \}$$
$$C_i = \begin{bmatrix} \beta_i & 0 & 0 & 0 & 1 \end{bmatrix}$$
$$C = \begin{bmatrix} C_1 & C_2 & \dots & C_N \end{bmatrix}$$
$$F_i = \begin{bmatrix} \frac{-1}{M_i} & 0 & 0 & 0 & 0 \\ \frac{-1}{M_i} & 0 & 0 & 0 & 0 \end{bmatrix}^T$$
$$F = diag\left\{ F_1 \quad F_2 \quad \dots \quad F_N \right\}$$

The ACE signal for each control area is the sum of Δf_i multiplied by β_i and the tie-line power exchange ΔP_{tie-i}, which is expressed by:

$$ACE_i = \beta_i \Delta f_i + \Delta P_{tie-i} \tag{2}$$

Next, the sliding-mode surface function can be constructed as:

$$s(t) = Gx(t) - \int_0^t G(A - BKC)x(\tau)d\tau \tag{3}$$

where G and K are constant matrices and G is selected to ensure matrix GB to be nonsingular.

For the ideal sliding-mode surface, the following function can be satisfied

$$s(t) = 0, \quad \dot{s}(t) = 0 \tag{4}$$

Then, substituting (1) and (4), the following equivalent sliding mode control law can be obtained

$$u_{eq}(t) = -KCx(t) - (GB)^{-1}GF\omega(t) \tag{5}$$

Therefore, the dynamic model (1) can be rewritten as:

$$\dot{x}(t) = Ax(t) - BKCx(t) + \tilde{F}\omega(t) \tag{6}$$

where $\tilde{F} = F - B(GB)^{-1}GF$.

The variations in system configuration and partly system failure will destroy the system stability. However, the Markov jump linear systems (MJLIs) can be applied to investigate the system stability caused by them [10]. The open communication network is structured as a Markov finite-state process with the following properties

$$P[r_s(t + \Delta t) = j | r_s(t) = i] = p_{ij}$$
$$0 \le i, j \le L, \ 0 \le \pi_{ij} \le 1, \ \sum_{j=0}^{L} \pi_{ij} = 1$$

where π_{ij} expresses the probability from mode i to mode j, as well as replace the probability of $r_s(t) = i$ to $r_s(t + \Delta t) = j$.

The system (1) can be further converted into the following Markov jump system as:

$$\dot{x}(t) = Ax(t) - BK_rCx(t) + \tilde{F}\omega(t) \tag{7}$$

For convenience of analysis, the $K(r(t))$ can be denoted as K_r.

Under network environment conditions, the sample data $ACE_i(t)$ cannot be used directly, as there are transmission time delays and data losses across communication networks. Therefore, taking the impact of networked environments into account. It is possible to write the input of the controller as:

$$y(t) = Cx(t_kh),\ t \in \left[t_kh + \tau_{t_k},\quad t_{k+1}h + \tau_{t_{k+1}} \right) \tag{8}$$

where t_kh is the transmitted instant of $x(t_kh)$; h means the constant sampling period. Only the network-induced transmission delays are considered as τ_{t_k}, $\tau_M = \max(\tau_{t_k})$, $d = \dot{\tau_{t_k}}$.

Since multi-area power systems sub-area are located in various locations. Hence, the multi-packet transmissions are needed. For the event-triggered scheme, when the defined triggering criteria are satisfied, the sampled signal packets can be transmitted. Throughout this scenario, the inefficient use of computational and communication resources can be reduced. And, the network bandwidth utilization can be maximized. In this subsection, the event-triggered transmission scheme can be rewritten as:

$$[x(t_kh + jh) - x(t_kh)]^T \Phi [x(t_kh + jh) - x(t_kh)] > \lambda x(t_kh)^T \Phi x(t_kh) \tag{9}$$

where Φ is an unknown positive matrix which need to be designed and $\lambda \in [0, 1)$.

The benefit of the event-triggered scheme is that the occurrence of a transmission is contingent on the threshold of the state-dependent. To improve this scheme performance, the following adaptive event-triggered scheme will be introduced into this paper:

$$[x(t_kh + jh) - x(t_kh)]^T \Phi [x(t_kh + jh) - x(t_kh)] > \lambda(t_kh) x(t_kh)^T \Phi x(t_kh) \tag{10}$$

Comparing with the predetermined time invariant λ in (9), the $\lambda(t_kh)$ in (10) can be adaptively modified according to the previous and present transmitted signal packets:

$$\lambda(t_kh) = \max(\lambda_m, \eta\lambda(t_{k-1}h)) \tag{11}$$

where $\lambda_m > 0$ and

$$\eta = \begin{cases} 0, & if\ \|x(t_kh)\| \geq \|x(t_{k-1}h)\| \\ 1 - \dfrac{2\alpha}{\pi} atan\left(\dfrac{\|x(t_kh)\| - \|x(t_{k-1}h)\|}{\|x(t_kh)\|}\right), & otherwise \end{cases}$$

Denote:

$$\begin{aligned} \Omega_0 &= [t_kh + \tau_{t_k},\ t_kh + h + \tau_M), \\ \Omega_j &= [t_kh + jh + \tau_M,\ t_kh + jh + h + \tau_M), \\ \Omega_{d_k} &= [t_kh + d_kh + \tau_M,\ t_{k+1}h + \tau_{t_{k+1}}), \quad (j = 1, 2, \ldots, d_k) \end{aligned}$$

So, there are

$$[t_kh + \tau_{t_k},\ t_{k+1}h + \tau_{t_{k+1}}) = \bigcup_{j=0}^{j=d_k} \Omega_j \tag{12}$$

At the same time, defining

$$e(t) = \begin{cases} 0, & k \in \Omega_0 \\ x(t_kh) - x(t_kh + mh), & k \in \Omega_m \\ x(t_kh) - x(t_kh + jh), & k \in \Omega_j \end{cases} \tag{13}$$

where $j = \sup\{m \in N | t_kh + mh < t_{k+1}h, m = 1, 2, \ldots\}$.

The real transmitted data under the adaptive event-triggered scheme (10) is

$$u(t) = Ky(t_kh) = KCx(t_kh) \tag{14}$$

On the whole, by utilizing the Markov jump theory, the multi-area power system model based on adaptive event-triggered SMC scheme can be described as the following linear time-invariant system

$$\dot{x}(t) = Ax(t) - BK_rCe(t) - BK_rCx(t - \tau_{t_k}) + \tilde{F}\omega(t) \tag{15}$$

Remark 1: It should be noted that the initial state output $x(0)$ is assumed to be successfully transmitted. Then, the release time instant of the rest state output will be determined by the next judgment scheme (10). Thus, the controller will be updated at its event time, so only a part of sampling information can be transmitted, which can effectively save the limited network resources.

Remark 2: The benefit of the event-triggered scheme is that the transmission of the signal packets depends on a state-dependent threshold relative to the period communication scheme. Additional, the adaptive parament $\lambda(t_kh)$ is considered in this paper,which can be adaptively modified according to the circumstances [21]. In this adaptive event-triggered scheme, the smaller $\lambda(t_{k+1}h)$ is applied to set more transmission signal packets, which can increase the transmission frequency. Meanwhile, the higher $\lambda(t_{k+1}h)$ will be utilized to set lower transmission frequency. In this way, it can save more communication bandwidth and improve network utilization.

The following lemmas are introduced in advance before presenting the main results.

Lemma 1 [36]: Let $Z_1 = Z_1^T$, $0 < Z_2 = Z_2^T$ and Z_3 be real matrices of appropriate dimensions, then $Z_1 + Z_3^T Z_2^{-1} Z_3 < 0$, if and only if

$$\begin{bmatrix} Z_1 & Z_3^T \\ Z_3 & -Z_2 \end{bmatrix} < 0 \quad \text{or} \quad \begin{bmatrix} -Z_2 & Z_3 \\ Z_3^T & Z_1 \end{bmatrix} < 0.$$

Lemma 2 [36]: For a given matrix $M > 0$, the following inequality holds for all continuously differentiable function x in $[a, b]$

$$\int_a^b \dot{x}^T(s) M \dot{x}(s) ds \geq \frac{1}{b-a}\zeta_1^T M \zeta_1 + \frac{3}{b-a}\zeta_2^T M \zeta_2,$$

where $\zeta_1 = x(b) - x(a)$ and $\zeta_2 = x(b) + x(a) - \frac{2}{b-a}\int_a^b x(s) ds$.

Lemma 3 [37]: For given positive integers n, m, a, scalar $\alpha \in (0, 1)$, an $n \times n$-matrix $R > 0$, two $n \times m$-matrices W_1,

W_2. Define, for all vector $\xi \in R^m$, the function $\Theta(\alpha, R)$ given by

$$\Theta(\alpha, R) = \frac{1}{\alpha}\xi^T {W_1}^T R W_1 \xi + \frac{1}{1-\alpha}\xi^T {W_2}^T R W_2 \xi.$$

If there is a matrix such that $\begin{bmatrix} R & * \\ X & R \end{bmatrix} > 0$, then the following inequality holds

$$\min_{\alpha\in(0,1)} \Theta(\alpha, R) \geq \begin{bmatrix} W_1\xi \\ W_2\xi \end{bmatrix}^T \begin{bmatrix} R & * \\ X & R \end{bmatrix} \begin{bmatrix} W_1\xi \\ W_2\xi \end{bmatrix}$$

Lemma 4 [37]: Given matrices $Q = Q^T$, H,E and $R = R^T > 0$ of appropriate dimensions, $Q+HFE+E^TF^TH^T < 0$ for all F satisfying $F^TF < R$, if and only if there exists some $\lambda > 0$ such that $Q + \lambda HH^T + \lambda^{-1}E^TRE < 0$.

III. MAIN RESULTS OF THE SLIDING MODE CONTROL AND ADAPTIVE EVENT-TRIGGERED SCHEME ON THE MARKOV MODEL OF POWER SYSTEM

In this section, the robust stability and stabilization results of the system (15) with the adaptive event-triggered sliding-mode control scheme and Markov model will be developed. Firstly, the robust stability results for the system (15) with $\omega(k) = 0$ will be presented. Then, taking disturbance into account, the robust H_∞ stability results for power system (15) will be developed. Finally, the sliding mode controller will be designed for system (15).

Theorem 1: For given positive constant $\varepsilon \in (0, 1)$, the system (15) with $\omega(k) = 0$ is asymptotically stable, if there exist positive definite matrices $P_r, Q_{1r}, Q_{2r}, S_r, T_r, \Phi$, appropriate dimensions $X_{1r}, X_{2r}, X_{3r}, X_{4r}, Y_r$ and identity matrix with appropriate dimensions I, such the following matrix inequalities hold for all $r = 1, \ldots, L$

$$\Pi_r = \begin{bmatrix} \Pi_{11r} & * & * & * \\ \Pi_{21r} & \Pi_{22r} & * & * \\ \Pi_{31r} & 0 & \Pi_{33r} & * \\ \Pi_{41r} & 0 & 0 & \Pi_{44r} \end{bmatrix} < 0 \quad (16)$$

$$X_r = \begin{bmatrix} S_r & * & * & * \\ 0 & 3S_r & * & * \\ X_{1r} & X_{3r} & S_r & * \\ X_{2r} & X_{4r} & 0 & 3S_r \end{bmatrix} > 0 \quad (17)$$

$$I < T_r \quad (18)$$

where

$$\begin{aligned}
\Pi_{11r} &= e_1^T \sum_{l=1}^{L} \pi_{rl} P_l e_1 + e_1^T Q_{1r} e_1 - (1-d) e_3^T Q_{1r} e_3 \\
&\quad + e_1^T Q_{2r} e_1 - e_4^T Q_{2r} e_4 - e_2^T \Phi e_2 + \lambda_m e_3^T \Phi e_3^T \\
&\quad - (e_1 - e_3)^T S_r (e_1 - e_3) \\
&\quad - (e_3 - e_4)^T S_r (e_3 - e_4) \\
&\quad - 3(e_1 + e_3 - 2e_5)^T S_r (e_1 + e_3 - 2e_5) \\
&\quad - 3(e_3 + e_4 - 2e_6)^T S_r (e_3 + e_4 - 2e_6) \\
&\quad - 2(e_3 - e_4)^T X_{1r} (e_1 - e_3) \\
&\quad - 2(e_3 - e_4)^T X_{3r} (e_1 + e_3 - 2e_5) \\
&\quad - 2(e_3 + e_4 - 2e_6)^T X_{2r} (e_1 - e_3) \\
&\quad - 2(e_3 + e_4 - 2e_6)^T X_{4r} (e_1 + e_3 - 2e_5) \\
\Pi_{21r} &= \Pi_{31r} = [(1,1) = \ldots = (L,1) = A, \\
(1,2) &= -BK_1C, \ldots, (L,2) = -BK_LC, \\
(1,3) &= -BK_1C, \ldots, (L,3) = -BK_LC] \\
\Pi_{22r} &= diag\{-\pi_{r1}\tau_M(S_1 - 2Y_1), \ldots, -\pi_{rL}\tau_M \\
&\quad \times (S_L - 2Y_L)\} \\
\Pi_{33r} &= diag\{-\varepsilon^{-1}\pi_{r1}(T_1 - 2Y_1), \ldots, -\varepsilon^{-1}\pi_{rL} \\
&\quad \times (T_L - 2Y_L)\} \\
\Pi_{41r} &= \begin{bmatrix} P_1^T & \ldots & P_L^T \end{bmatrix}^T, \\
\Pi_{44r} &= diag\{-\varepsilon\pi_{r1}, \ldots, -\varepsilon\pi_{rL}\}
\end{aligned}$$

Proof: Define the Lyapunov function as:

$$\begin{aligned}
V(t) &= x^T(t) P_r x(t) + \int_{t-\tau_{t_k}}^{t} x^T(s) Q_{1r} x(s) ds \\
&\quad + \int_{t-\tau_M}^{t} x^T(s) Q_{2r} x(s) ds \\
&\quad + \tau_M \int_{-\tau_M}^{0} \int_{t+\theta}^{t} x^T(s) S_r x(s) ds d\theta
\end{aligned} \quad (19)$$

where P_r, Q_{1r}, Q_{2r}, S_r are positive-definite matrices with appropriate dimensions.

Calculating the derivative of (19) along the trajectory (15) with $\omega(k) = 0$, one has:

$$\begin{aligned}
\Delta V(t) &= 2\dot{x}^T(t) P_r x(t) + x^T(t) \sum_{l=1}^{L} \pi_{rl} P_l x(t) \\
&\quad + x^T(t) Q_{1r} x(t) + \sum_{l=1}^{L} \pi_{rl} [Ax(t) - BK_r Ce(t) \\
&\quad - BK_r Cx(t - \tau_{t_k})]^T P_l x(t) + x^T(t) Q_{2r} x(t) \\
&\quad + \sum_{l=1}^{L} \pi_{rl} x^T(t) P_l \cdot [Ax(t) - BK_r Ce(t) \\
&\quad - BK_r Cx(t - \tau_{t_k})] + x^T(t) \sum_{l=1}^{L} \pi_{rl} P_l x(t) \\
&\quad - (1-d) x^T(t - \tau_{t_k}) Q_{1r} x(t - \tau_{t_k}) \\
&\quad - x^T(t - \tau_M) Q_{1r} x(t - \tau_M) \\
&\quad + \tau_M \dot{x}^T(t) \sum_{i=1}^{L} \pi_{rl} S_l \dot{x}(t) \\
&\quad - \tau_M \int_{t-\tau_M}^{t} \dot{x}^T(s) S_r \dot{x}(s) ds
\end{aligned}$$

By utilizing Wirtinger-based inequality, $-\tau_M \int_{t-\tau_M}^{t} \dot{x}^T(s) S_r \dot{x}(t) ds$ can be rewritten as:

$$-\tau_M \int_{t-\tau_{t_k}}^{t} \dot{x}^T(s) S_r \dot{x}(t) ds$$

$$-\tau_M \int_{t-\tau_M}^{t-\tau_{t_k}} \dot{x}^T(s) S_r \dot{x}(t) ds$$
$$\leq -\frac{\tau_M}{\tau_{t_k}} W^T{}_{1r} \hat{S}_r W_{1r} - \frac{\tau_M}{\tau_M - \tau_{t_k}} W^T{}_{2r} \hat{S}_r W_{2r}$$

where

$$W_{1r} = [x(t) - x(t-\tau_{t_k});$$
$$x(t) + x(t-\tau_{t_k}) - \frac{2}{\tau_{t_k}} \int_{t-\tau_{t_k}}^{t} x(s) ds],$$
$$W_{2r} = [x(t-\tau_{t_k}) - x(t-\tau_M); x(t-\tau_{t_k})$$
$$+x(t-\tau_M) - \frac{2}{\tau_M - \tau_{t_k}} \int_{t-\tau_M}^{t-\tau_{t_k}} x(s) ds],$$
$$\hat{S}_r = diag\{S_r, 3S_r\}.$$

Defining the following augmenting state variable

$$\xi(t) = \Big[x(t) \quad e(t) \quad x(t-\tau_{t_k}) \quad x(t-\tau_M)$$
$$\frac{1}{\tau_{t_k}} \int_{t-\tau_{t_k}}^{t} x(m) dm \quad \frac{1}{\tau_M - \tau_{t_k}} \int_{t-\tau_M}^{t-\tau_{t_k}} x(m) dm \Big]^T$$

and $e_j = [\underbrace{0 \ldots 0}_{j-1}, 1, \underbrace{0 \ldots 0}_{6-j}], (j = 1, \ldots, 6).$

Under the adaptive event-triggered schem (10) condition, by applying Lemma 3, it follows that

$$\Delta V(t) - e(t)^T \Phi e(t) + \lambda_m x(t-\tau_{t_k})^T \Phi x(t-\tau_{t_k})$$
$$\leq \xi^T(k) \Omega_r \xi(k) < 0 \quad (20)$$

where

$$\Omega_r = \Pi_{11r} + \sum_{l=1}^{L} [Ae_1 - BK_l Ce_2 - BK_l Ce_3]^T \pi_{rl} P_l$$
$$+ \sum_{l=1}^{L} \pi_{rl} P_l [Ae_1 - BK_l Ce_2 - BK_l Ce_3]$$
$$+\tau_M \sum_{l=1}^{L} [Ae_1 - BK_l Ce_2 - BK_l Ce_3]^T$$
$$\times \pi_{rl} S_l [Ae_1 - BK_l Ce_2 - BK_l Ce_3]$$

Because $\Omega_r < 0$ and by utilizing Lemma 4, (17), (18) and the next condition can be obtained

$$\Pi_{11r} + \varepsilon \sum_{l=1}^{L} \pi_{rl} P_l^T P_l + \tau_M \sum_{l=1}^{L} [A_l e_1 - B_l K_l Ce_2$$
$$-B_l K_l Ce_3]^T \pi_{rl} R_l [A_l e_1 - B_l K_l Ce_2 - B_l K_l Ce_3]$$
$$+\varepsilon^{-1} \sum_{l=1}^{L} \pi_{rl} [A_l e_1 - B_l K_l Ce_2 - B_l K_l Ce_3]^T$$
$$\times T_l [A_l e_1 + B_l K_l Ce_2 - B_l K_l Ce_3] < 0$$

where T_r expresses positive definite matrices.

There is a fact that if the $Z < 0$, and $Y^T = Y$ can be satisfied, the $Y^T Z Y \leq -2Y - Z^{-1}$ can be obtained. By utilizing this fact and Lemma 1, condition (16), (17), and (18) can be obtained. Obviously, if $\Omega_r < 0$ can be satisfied, then $\Delta V(t) < \xi^T(t) \Omega_r \xi(t) < -\kappa \|\xi(t)\|^2 < 0$ can be obtained for a sufficiently small constant $\kappa > 0$. Therefore, system (15) with $\omega(t) = 0$ is asymptotically stable, and this completes the proof.

Remark 3: It should be noted that the inequalities scaling method is applied in this theorem. Thus, the conservative problem needs to be considered. In this theorem, the $-\tau_M \int_{t-\tau_M}^{t} \dot{x}^T(s) S_r \dot{x}(t) ds$ is rewritten as $-\tau_M \int_{t-\tau_{t_k}}^{t} \dot{x}^T(s) S_r \dot{x}(t) ds r - \tau_M \int_{t-\tau_M}^{t-\tau_{t_k}} \dot{x}^T(s) S_r \dot{x}(t) ds$. Then, Wirtinger-based inequality is employed in this derivation. In this way, the less conservative results can be expected than the existing research using Jensen inequality [6], [7].

Theorem 2: For given positive constant $\varepsilon \in (0, 1)$, the system (15) is asymptotically stable with H_∞ prescribed attention level γ, if there exist positive definite matrices P_r, Q_{1r}, Q_{2r}, S_r, T_r, Φ and appropriate dimensions X_{1r}, X_{2r}, X_{3r}, X_{4r}, Y_r such the following matrix inequalities hold for all $r = 1, \ldots, L$

$$\Pi'_r = \begin{bmatrix} \Pi'_{11r} & * & * & * \\ \Pi'_{21r} & \Pi_{22r} & * & * \\ \Pi'_{31r} & 0 & \Pi_{33r} & * \\ \Pi_{41r} & 0 & 0 & \Pi_{44r} \end{bmatrix} < 0 \quad (21)$$
$$X_r > 0, I < T_r$$

where

$$\Pi'_{11r} = e_7^T \sum_{l=1}^{L} \pi_{rl} P_l e_7 + e_7^T Q_{1r} e_7 + e_7^T Q_{2r} e_7$$
$$-(1-\tau_{t_k}) e_9^T Q_{1r} e_9 - e_{10}^T Q_{2r} e_{10}$$
$$+e_7^T C^T C e_7 - \gamma^2 e_{11}^T e_{11} - e_8^T \Phi e_8$$
$$+\lambda_m e_9^T \Phi e_9 - (e_1 - e_3)^T S_r (e_7 - e_9)$$
$$-3(e_7 + e_9 - 2e_{12})^T S_r (e_7 + e_9 - 2e_{12})$$
$$-2(e_9 - e_{10})^T X_{1r} (e_7 - e_9)$$
$$-2(e_9 - e_{10})^T X_{3r} (e_7 + e_9 - 2e_{12})$$
$$-(e_9 - e_{10})^T S_r (e_9 - e_{10})$$
$$-2(e_9 + e_{10} - 2e_{13})^T X_{2r} (e_7 - e_9)$$
$$-2(e_9 + e_{10} - 2e_{13})^T X_{4r} (e_7 + e_9 - 2e_{12})$$
$$-3(e_9 + e_{10} - 2e_{13})^T S_r (e_9 + e_{10} - 2e_{13})$$
$$\Pi'_{21r} = \Pi'_{31r} = [(1,1) = \ldots = (L,1) = A,$$
$$(1,2) = -BK_1 C, \ldots, (L,2) = -BK_L C,$$
$$(1,3) = -BK_1 C, \ldots, (L,3) = -BK_L C,$$
$$(1,5) = \ldots = (L,5) = \tilde{F}]$$

Proof: For a specified attenuation level $\gamma > 0$, the cost function J can be interpreted as:

$$J = \int_0^\infty y^T(t) y(t) - \gamma^2 \omega^T(t) \omega(t) dt \quad (22)$$

Under the adaptive event-triggered scheme, and for $\omega(t) \in l_2[0, \infty]$ and $t > 0$ condition, one gets

$$J \leq y^T(t) y(t) - \gamma^2 \omega^T(t) \omega(t) + \Delta V(t)$$
$$-e(t)^T \Phi e(t) + \lambda_m x(t-\tau_{t_k})^T \Phi x(t-\tau_{t_k})$$

Then one further has

$$\begin{aligned} y^T(t)y(t) &- \gamma^2\omega^T(t)\omega(t) + \Delta V(t) - e(t)^T\Phi e(t) \\ &+ \lambda_m x(t-\tau_{t_k})^T\Phi x(t-\tau_{t_k}) \\ &< 0 \end{aligned} \tag{23}$$

Defining the augmenting variable as:

$$\xi(t)' = \left[x(t) \quad e(t) \quad x(t-\tau_{t_k}) \quad x(t-\tau_M) \quad \omega(t) \quad \frac{1}{\tau_{t_k}}\int_{t-\tau_{t_k}}^{t} x(m)dm \quad \frac{1}{\tau_M-\tau_{t_k}}\int_{t-\tau_M}^{t-\tau_{t_k}} x(m)dm\right]^T$$

and $e_j = [\underbrace{0\ldots0}_{j-7}, 1, \underbrace{0\ldots0}_{13-j}], \quad (j = 7, \ldots, 13).$

The condition (23) can be calculated by

$$\xi'^T(k)\Omega'_r\xi'(k) < 0 \tag{24}$$

where

$$\begin{aligned} \Omega'_r = \Pi'_{11r} &+ \sum_{l=1}^{L}[Ae_7 - BK_lCe_8 - BK_lCe_9 \\ &+\tilde{F}_le_{11}]^T\pi_{rl}P_l + \sum_{l=1}^{L}\pi_{rl}P_l[Ae_7 - BK_lCe_8 - BK_lCe_9 \\ &+\tilde{F}e_{11}] + \tau_M\sum_{l=1}^{L}[Ae_7 - BK_lCe_8 - BK_lCe_9 + \tilde{F}e_{11}]^T \\ &\pi_{rl}S_l[Ae_7 - BK_lCe_8 - BK_lCe_9 + \tilde{F}e_{11}] \end{aligned}$$

By utilizing the same method proposed in Theorem 1, and combining Lemma 1 and Lemma 3, then condition (21) can be obtained. Finally, if $\Omega'_r < 0$, so $J < -\kappa\left\|\xi'_1(t)\right\|^2 < 0$ can be satisfied, and the condition (21) will be obtained. Therefore, the power system (15) is H_∞ stable with performance index γ. Then, the proof of this theorem can be completed.

Remark 4: It should be noted that the feasible solution of the controller gain and H_∞ prescribed attention level γ can be obtained. However, those results are not strictly for this system. To solve the optimal attenuation level γ, the following constrained optimization problem can be obtained as:

$$\min \quad \delta \qquad s.t. \begin{cases} \Pi'_r < 0, & X_r > 0,\ I < T_r \\ P_r > 0, & Q_{1r} > 0, Q_{2r} > 0, \\ S_r > 0, & \Phi > 0 \end{cases}$$

where $\delta = \gamma^2$.

Remark 5: In Theorem 2, the robust H_∞ stability results for system (15) under conservative condition are developed. And the adaptive event-triggered sliding mode controller gain can be obtained. Then, an constrained optimization problem is proposed to solve the optimal attenuation level γ and time delay τ_M. In the beginning, the small time delay need be started as the initialization, and by decreasing τ_M in every iteration and $\tau_M = \tau_M + \Delta\tau$ until the constrained optimization problem cannot find the feasibility results.

TABLE 2. Parameters of the three-area LFC scheme.

Area	R	M	D	T_g	T_{ch}
1	0.05	10.0	1.0	0.1	0.3
2	0.05	12.0	1.5	0.17	0.4
3	0.05	12.0	1.8	0.2	0.35
	$T_{12} = 0.52$		$T_{13} = 0.55$	$T_{23} = 0.47$	

It is noted that the H_∞ stability results and controller gain for power system (15) are all discussed in the above. Next, the SMC strategy will be exhibited in the Theorem 3 below.

Theorem 3: The sliding mode surface function can be designed as (3). To ensure the $s(t)\dot{s}(t) < 0$ reaching condition is satisfied, the decentralized switching control law can be built as:

$$u(t) = -KCx(t) - k_1(GB)^{-1}\left\|G\hat{F}\right\|(sgn(s(t)) + s(t)) \tag{25}$$

where

$$sgn(s(t)) = \begin{cases} -1, & if\ s(t) < 0 \\ 0, & if\ s(t) = 0 \\ 1, & if\ s(t) > 0 \end{cases}$$

Proof: The Lyapunov function can be constructed as:

$$V(t) = \frac{1}{2}s^T(t)s(t) \tag{26}$$

Then, combining (1) and (25), $\dot{V}(t) < 0$ can be further obtained. Besides, one can infer that the built controller will guarantee the reaching state. Therefore, the built controller (25) will move the system (15) to the sliding surface (3). Then, a sliding motion can be maintained afterward. Based on the SMC theory, the closed-loop system developed by applying the control law (25) to the (15) is asymptotically stable.

IV. CASE STUDY AND DISCUSSION

In this section, to demonstrate the effectiveness of the presented adaptive event-triggered SMC scheme for a multi-area power system under a networked environment, the simulation cases of the three-area power system is proposed. At first, the availability of the designed controller and release intervals results of the built adaptive event-triggered scheme are presented. Then, the comparison results of minimum H_∞ prescribed attention level γ obtained in this paper with the results obtained in [18] are exhibited in the second case.

A. FREQUENCY DEVIATION AND RELEASE INTERVALS RESULTS

To demonstrate the availability and effectiveness of the proposed method, a three-area power system is carried out in this case study, as shown in Fig. 2. Meanwhile, the parameters of this model are listed in Table 2:

The transition probability matrix is set as follows

$$P = \begin{bmatrix} 0.5088 & 0.4912 \\ 0.4286 & 0.5714 \end{bmatrix}$$

and it is plotted in Fig. 3 (a).

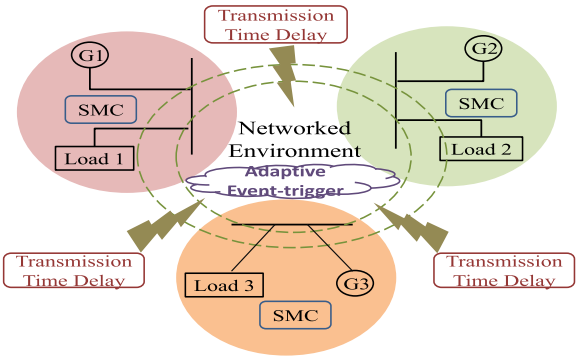

FIGURE 2. A three-area restructured power system.

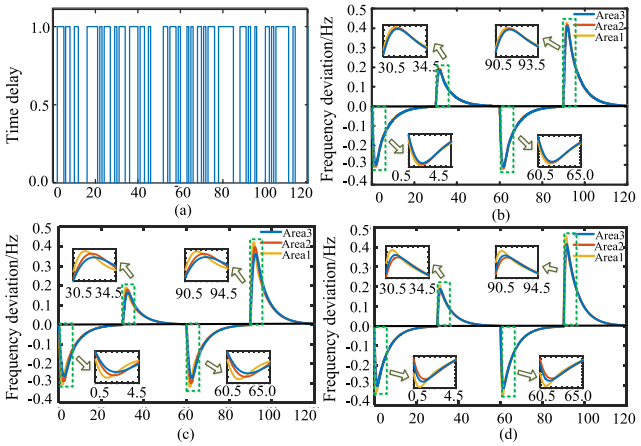

FIGURE 3. Results of case study: (a) Random transmission delay, (b) Frequency deviations with step load disturbances, (c) Frequency deviations with +50% parameter uncertainty, (d) Frequency deviations with −50% parameter uncertainty.

By solving remark 4 with $G = [-1\ 1\ -1\ 1\ 1]$, $\lambda_m = 0.01$, $d = 0.5$, $k_1 = 1.0$, the following control law can be calculated

$$K_{11}(t) = -0.0391, \quad K_{12}(t) = -0.0392,$$
$$K_{21}(t) = -0.0452, \quad K_{22}(t) = -0.0456,$$
$$K_{31}(t) = -0.0926, \quad K_{32}(t) = -0.0941$$

By utilizing the Matlab/Simulink Toolbox, the frequency response curves of all areas are illustrated in Fig. 3 (b). In this case, the total simulation time is 120s, and four random successive load disturbances are exhibited, which at 0s, 30s, 60s, and 90s, respectively. One can conclude that the multi-area power can be well stabilized under the proposed adaptive event-triggered SMC scheme. Meanwhile, the desired control performance can be maintained. As shown in Fig. 3 (b), the system frequency deviation Δf_i for all the three areas can be brought back to zero after a finite time. It is demonstrated that by utilizing the proposed adaptive event-triggered SMC scheme, the stability of the multi-area power system can be restored.

To exhibit the efficacy of the proposed adaptive event-triggered SMC scheme further, the robustness of this

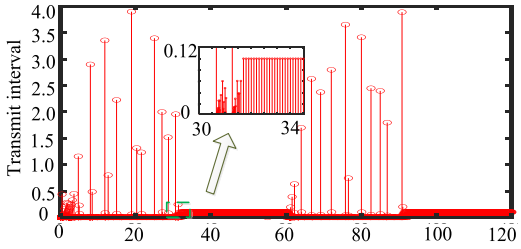

FIGURE 4. Release instant and release intervals for Area 3 with $\lambda_m = 0.01$.

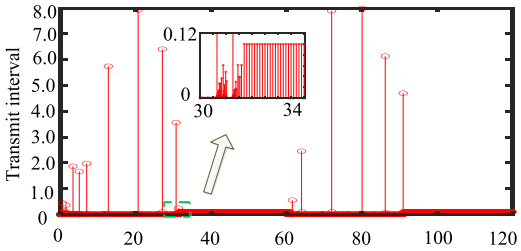

FIGURE 5. Release instant and release intervals for Area 3 with $\lambda_m = 0.5$.

TABLE 3. Number of trigger times under different schemes.

λ_m	0.0	0.1	0.3	0.6
[18]	1200	888	408	360
This paper	1200	343	283	258

system with the case of +50% parameter uncertainty and −50% parameter uncertainty will be applied. Fig. 3 (c) and Fig. 3 (d) illustrate the Δf_i of three areas under +50% and −50% parameter uncertainty condition, respectively. It can be inferred that all the three areas' Δf_i can also be brought back to zero after a finite time under the parameter uncertainty condition. Consequently, it can be claimed that the proposed approach provides excellent robustness.

To certify the availability of the proposed adaptive event-triggered scheme, the release intervals and the number of transmitted packets with $\lambda_m = 0.01$ and $\lambda_m = 0.5$ are exhibited in Fig. 4 and Fig. 5, respectively. For different triggered parameter λ given in [18], the number of transmitted packets are described in Table 3, respectively. It can be concluded that the number of packets transmitted with the proposed adaptive event-trigger is smaller than those results in [18]. Besides, it can be inferred when the adaptive time invariant $\lambda(t_k h)$ becomes larger, the smaller amount of sampled data is needed to transmit.

It should be pointed out that in the above comparisons, the effectiveness of the time delay is not taken into account in [18], however, it is considered in this paper. In this way, the effectiveness of the exhibited adaptive event-triggered SMC scheme can be shown.

B. MINIMUM H_∞ PRESCRIBED ATTENTION LEVEL γ

To demonstrate the conservative of the results, caused by the application of inequalities scaling, a two-area power system is further considered in this case. The parameters are the same as those in [38] as shown in Table 4.

TABLE 4. Parameters of the two-area LFC scheme.

Area	R	M	D	T_g	T_{ch}
1	0.05	10.0	1.0	0.1	0.3
2	0.05	12.0	1.5	0.4	0.17
	$T_{12} = 0.1986$				

TABLE 5. Comparison of minimum disturbance attenuation level γ.

Method	Disturbance Attenuation Level γ
[38]	0.4493
This paper	0.2541

Setting $G = [-1\ 1\ -1\ 1\ 1]$, $\lambda_m = 0.1$ and $d = 0.5$. By utilizing the proposed interrelated algorithm, the minimum disturbance attenuation level γ for the proposed Remark 4 and some other methods in [38] are presented in Table 5. As Table 5 shown, the disturbance attenuation level γ obtained in this paper is smaller than the results in [38]. It can be demonstrated that the result obtained in this paper is less conservative than the result obtained in [38], which shows the effectiveness of the proposed method.

V. CONCLUSION

In this paper, the adaptive event-triggered SMC of LFC for a multi-area power system has been proposed under open network environment conditions. The simulations have demonstrated the exhibited adaptive event-triggered scheme can save more network resources and maximize network bandwidth utilization. It has been manifested that the proposed adaptive event-triggered SMC scheme expresses better robustness towards $+50\%$ and -50% parameter uncertainty and external disturbances rejection capability. Based on the uncertainty parameter and external disturbances condition, the Markov jump linear model has been proposed to describe the LFC scheme for the multi-area power system. Moreover, by utilizing the Wirtinger-based inequality and Lyapunov theory, the robust stability and stabilization criteria with less conservatism have been built. Therefore, the designed scheme can ensure the desired system performance and reduce the communication burden has been illustrated by examples and simulations.

REFERENCES

[1] S. Kayalvizhi and D. M. Vinod Kumar, "Load frequency control of an isolated micro grid using fuzzy adaptive model predictive control," *IEEE Access*, vol. 5, pp. 16241–16251, 2017.

[2] B. Polajzer, M. Petrun, and J. Ritonja, "Adaptation of load-frequency-control target values based on the covariances between area-control errors," *IEEE Trans. Power Syst.*, vol. 33, no. 6, pp. 5865–5874, Nov. 2018.

[3] Y. Xu, C. Li, Z. Wang, N. Zhang, and B. Peng, "Load frequency control of a novel renewable energy integrated micro-grid containing pumped hydropower energy storage," *IEEE Access*, vol. 6, pp. 29067–29077, Apr. 2018.

[4] C. Chen, M. Cui, X. Wang, K. Zhang, and S. Yin, "An investigation of coordinated attack on load frequency control," *IEEE Access*, vol. 6, pp. 30414–30423, 2018.

[5] C. Chen, K. Zhang, K. Yuan, L. Zhu, and M. Qian, "Novel detection scheme design considering cyber attacks on load frequency control," *IEEE Trans. Ind. Informat.*, vol. 14, no. 5, pp. 1932–1941, May 2018.

[6] H. A. Yousef, K. AL-Kharusi, M. H. Albadi, and N. Hosseinzadeh, "Load frequency control of a multi-area power system: An adaptive fuzzy logic approach," *IEEE Trans. Power Syst.*, vol. 29, no. 4, pp. 1822–1830, Jul. 2014.

[7] S. Saxena and Y. V. Hote, "Load frequency control in power systems via internal model control scheme and model-order reduction," *IEEE Trans. Power Syst.*, vol. 28, no. 3, pp. 2749–2757, Aug. 2013.

[8] T. Masuta and A. Yokoyama, "Supplementary load frequency control by use of a number of both electric vehicles and heat pump water heaters," *IEEE Trans. Smart Grid*, vol. 3, no. 3, pp. 1253–1262, Sep. 2012.

[9] Y. Zhao, A. Fatehi, and B. Huang, "A data-driven hybrid ARX and Markov chain modeling approach to process identification with time-varying time delays," *IEEE Trans. Ind. Electron.*, vol. 64, no. 5, pp. 4226–4236, May 2017.

[10] L. Cai, Z. He, and H. Hu, "A new load frequency control method of multi-area power system via the viewpoints of port-Hamiltonian system and cascade system," *IEEE Trans. Power Syst.*, vol. 32, no. 3, pp. 1689–1700, May 2017.

[11] L. Xiong, H. Li, and J. Wang, "LMI based robust load frequency control for time delayed power system via delay margin estimation," *Int. J. Electr. Power Energy Syst.*, vol. 100, pp. 91–103, Sep. 2018.

[12] S. Wen, X. Yu, Z. Zeng, and J. Wang, "Event-triggering load frequency control for multiarea power systems with communication delays," *IEEE Trans. Ind. Electron.*, vol. 63, no. 2, pp. 1308–1317, Feb. 2016.

[13] V. Léchappé, E. Moulay, F. Plestan, and Q.-L. Han, "Discrete predictor-based event-triggered control of networked control systems," *Automatica*, vol. 107, pp. 281–288, Sep. 2019.

[14] M. Li, J. Zhao, J. Xia, G. Zhuang, and W. Zhang, "Extended dissipative analysis and synthesis for network control systems with an event-triggered scheme," *Neurocomputing*, vol. 312, pp. 34–40, Oct. 2018.

[15] C. Peng, J. Li, and M. Fei, "Resilient event-triggering H_∞ load frequency control for multi-area power systems with energy-limited DoS attacks," *IEEE Trans. Power Syst.*, vol. 32, no. 5, pp. 4110–4118, Sep. 2017.

[16] Z.-G. Wu, Y. Xu, Y.-J. Pan, H. Su, and Y. Tang, "Event-triggered control for consensus problem in multi-agent systems with quantized relative state measurements and external disturbance," *IEEE Trans. Circuits Syst. I, Reg. Papers*, vol. 65, no. 7, pp. 2232–2242, Jul. 2018.

[17] P. Dahiya, P. Mukhija, and A. R. Saxena, "Design of sampled data and event-triggered load frequency controller for isolated hybrid power system," *Int. J. Electr. Power Energy Syst.*, vol. 100, pp. 331–349, Sep. 2018.

[18] X. Su, X. Liu, and Y.-D. Song, "Event-triggered sliding-mode control for multi-area power systems," *IEEE Trans. Ind. Electron.*, vol. 64, no. 8, pp. 6732–6741, Aug. 2017.

[19] L. Dong, Y. Tang, H. He, and C. Sun, "An event-triggered approach for load frequency control with supplementary ADP," *IEEE Trans. Power Syst.*, vol. 32, no. 1, pp. 581–589, Jan. 2017.

[20] Y. Fan, G. Hu, and M. Egerstedt, "Distributed reactive power sharing control for microgrids with event-triggered communication," *IEEE Trans. Control Syst. Technol.*, vol. 25, no. 1, pp. 118–128, Jan. 2017.

[21] H. Li, X. Wang, and J. Xiao, "Adaptive event-triggered load frequency control for interconnected microgrids by observer-based sliding mode control," *IEEE Access*, vol. 7, pp. 68271–68280, May 2019.

[22] W. Li, Z. Xie, P. K. Wong, X. Mei, and J. Zhao, "Adaptive-Event-Trigger-Based fuzzy nonlinear lateral dynamic control for autonomous electric vehicles under insecure communication networks," *IEEE Trans. Ind. Electron.*, early access, Feb. 7, 2020, doi: 10.1109/TIE.2020.2970680.

[23] H. Du, X. Chen, G. Wen, X. Yu, and J. Lu, "Discrete-time fast terminal sliding mode control for permanent magnet linear motor," *IEEE Trans. Ind. Electron.*, vol. 65, no. 12, pp. 9916–9927, Dec. 2018.

[24] B. Yang, T. Yu, H. Shu, Y. Zhang, J. Chen, Y. Sang, and L. Jiang, "Passivity-based sliding-mode control design for optimal power extraction of a PMSG based variable speed wind turbine," *Renew. Energy*, vol. 119, pp. 577–589, Apr. 2018.

[25] K. Mei and S. Ding, "Second-order sliding mode controller design subject to an upper-triangular structure," *IEEE Trans. Syst., Man, Cybern. Syst.*, pp. 1–11, 2019, doi: 10.1109/TSMC.2018.2875267.

[26] Y. Mi, X. Hao, Y. Liu, Y. Fu, C. Wang, P. Wang, and P. C. Loh, "Sliding mode load frequency control for multi-area time-delay power system with wind power integration," *IET Gener., Transmiss. Distrib.*, vol. 11, no. 18, pp. 4644–4653, Dec. 2017.

[27] S. Ding, J. H. Park, and C.-C. Chen, "Second-order sliding mode controller design with output constraint," *Automatica*, vol. 112, Feb. 2020, Art. no. 108704, doi: 10.1016/j.automatica.2019.108704.

[28] Y. Sun, Y. Wang, Z. Wei, G. Sun, and X. Wu, "Robust H_∞ load frequency control of multi-area power system with time delay: A sliding mode control approach," *IEEE/CAA J. Automatica Sinica*, vol. 5, no. 2, pp. 610–617, Mar. 2018.
[29] Y. Mi, Y. Fu, D. Li, C. Wang, P. C. Loh, and P. Wang, "The sliding mode load frequency control for hybrid power system basedon disturbance observer," *Int. J. Elec. Power*, vol. 74, pp. 446–452, Jan. 2016.
[30] B. Yang, T. Yu, H. Shu, J. Dong, and L. Jiang, "Robust sliding-mode control of wind energy conversion systems for optimal power extraction via nonlinear perturbation observers," *Appl. Energy*, vol. 210, pp. 711–723, Jan. 2018.
[31] J. W. Choi, S. Y. Heo, and M. K. Kim, "Hybrid operation strategy of wind energy storage system for power grid frequency regulation," *IET Gener., Transmiss. Distrib.*, vol. 10, no. 3, pp. 736–749, Feb. 2016.
[32] M. Shen, S. K. Nguang, C. K. Ahn, and Q.-G. Wang, "Robust H_2 control of linear systems with mismatched quantization," *IEEE Trans. Autom. Control*, vol. 64, no. 4, pp. 1702–1709, Apr. 2019.
[33] S. Sou, W. Lin, K. Lan, and C. Lin, "Indoor location learning over wireless fingerpringting system with particle Markov chain model," *IEEE Trans. Syst. Man Cybern. Syst.*, vol. 49, no. 9, pp. 1901–1911, Sep. 2019.
[34] M. Shen, S. K. Nguang, and C. K. Ahn, "Quantized H_∞ output control of linear Markov jump systems in finite frequency domain," *IEEE Access*, vol. 7, pp. 8713–8725, Jan. 2019.
[35] G. Ioannou, P. Louvieris, and N. Clewley, "A Markov multi-phase transferable belief model for cyber situational awareness," *IEEE Access*, vol. 7, pp. 39305–39320, 2019.
[36] A. Seuret and F. Gouaisbaut, "Wirtinger-based integral inequality: Application to time-delay systems," *Automatica*, vol. 49, no. 9, pp. 2860–2866, Sep. 2013.
[37] P. T. Nam, P. N. Pathirana, and H. Trinh, "Discrete wirtinger-based inequality and its application," *J. Franklin Inst.*, vol. 352, no. 5, pp. 1893–1905, May 2015.
[38] Y. Sun, N. Li, X. Zhao, Z. Wei, G. Sun, and C. Huang, "Robust H_∞ load frequency control of delayed multi-area power system with stochastic disturbances," *Neurocomputing*, vol. 193, pp. 58–67, Jun. 2016.

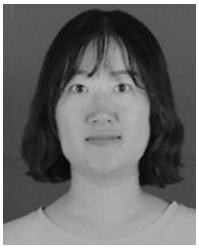

XINXIN LV (Student Member, IEEE) received the B.S. degree in mathematics from Ludong University, in 2015. She is currently pursuing the Ph.D. degree in electrical engineering with Hohai University, China. From 2019 to 2020, she was a joint Ph.D. Student with RTX Laboratory, University of Alberta, Edmonton, AB, Canada. Her research interests include power system modeling and application, stability analysis and control of power systems, and load frequency control of power systems.

YONGHUI SUN (Member, IEEE) received the Ph.D. degree from the City University of Hong Kong, Hong Kong, in 2010. He is currently a Professor with the College of Energy and Electrical Engineering, Hohai University. He has authored over 60 articles in refereed international journals. His current research interests include stability analysis and control of power systems, optimal planning and operation of integrated energy systems, optimization algorithms, and data analysis. He was a recipient of the First Award of Jiangsu Provincial Progress in Science and Technology, in 2010, as a Fourth Project Member. He is an active reviewer for many international journals.

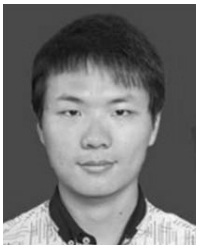

YI WANG (Student Member, IEEE) received the B.S. degree from the Luoyang Institute of Science and Technology, Luoyang, China, in 2014. He is currently pursuing the Ph.D. degree in electrical engineering with Hohai University, Nanjing, China. He was with the University of Alberta, Canada, as a joint Ph.D. Student, from 2018 to 2019. His research interests include theoretical and algorithmic studies in power system state estimation, parameters identification, power system dynamics, signal processing, and cyber security.

VENKATA DINAVAHI (Fellow, IEEE) received the B.Eng. degree in electrical engineering from the Visvesvaraya National Institute of Technology, Nagpur, India, in 1993, the M.Tech. degree in electrical engineering from the Indian Institute of Technology, Kanpur, India, in 1996, and the Ph.D. degree in electrical and computer engineering from the University of Toronto, Toronto, ON, Canada, in 2000. He is currently a Professor with the Department of Electrical and Computer Engineering, University of Alberta, Edmonton, AB, Canada. His research interests include real-time simulation of power systems and power electronic systems, electromagnetic transients, device-level modeling, large-scale systems, and parallel and distributed computing.